Limnol. Oceanogr., 58(1), 2013, 193–202

doi:10.4319/lo.2013.58.1.0193

Trait-based models of nutrient uptake in microbes extend the Michaelis-Menten framework

Øyvind Fiksen,[a,b,*] Michael J. Follows,[c] and Dag L. Aksnes [a]

[a] Department of Biology, University of Bergen, Bergen, Norway
[b] Uni Research, Bergen, Norway
[c] Earth, Atmospheric, and Planetary Sciences, Massachusetts Institute of Technology, Cambridge, Massachusetts

Abstract

In microbial competition theory, the Michaelis-Menten (MM) half-saturation coefficient is often considered to be a trait of an organism defining competitive strength in a trade-off conflict with maximum uptake rate. Theoretical studies have shown that a quadratic model characterizes the uptake rate, and that this model can be approximated by a MM model. Here, we review recent developments in nutrient uptake modeling with particular emphasis on cell size, uptake sites, and molecular diffusion. We quantify the bias of the MM approximation to be up to 50% in some configurations. More importantly, we find no mechanistic foundation for a trade-off conflict between the half-saturation coefficient and the maximum specific uptake rate. Measured MM coefficients need to be interpreted in an extended framework where nutrient uptake is explicitly parameterized in terms of cell size, uptake sites, and molecular diffusion. This provides a richer and more mechanistic picture of the way in which uptake rate varies with traits of the organism and environmental variables. Estimates of these key traits can be obtained from measured properties like affinity, the MM half saturation coefficient, and the maximum uptake rate. Using recent estimates of allometric scaling of MM coefficients, we find that handling time, uptake site density, and specific affinity decrease with cell size. Unlike the half-saturation coefficient, specific affinity is a consistent and meaningful measure of competitive strength of microbes, but it is not in a trade-off conflict with maximum uptake rate if the cell is surrounded by a diffusive boundary layer.

Early work with chemostats extended the Michaelis-Menten (MM) enzyme kinetics to growth of whole organisms such as bacteria (Monod 1949). Later, Dugdale (1967) introduced MM to represent the effect of nutrient concentration on phytoplankton uptake rate (V):

$$V = V_{\max} \frac{S_\infty}{K_\infty + S_\infty} \quad (1)$$

where S_∞ is the measured bulk nutrient concentration outside the boundary layer of the cell, $V_{\max}$ is the maximal uptake rate, and K_∞ is the MM bulk half-saturation coefficient, which is the observed bulk nutrient concentration (S_∞) when the uptake rate is 50% of $V_{\max}$ (Table 1). This equation has become the standard representation of nutrient-limited uptake and growth in classical competition theory as well as for modern ocean ecosystem models. In competition theory, K_∞ frequently appears as a constant reflecting a particular species (Tilman 1977), and in modern terms, it is often considered to be a trait that defines its competitive strength at low nutrient concentrations (Litchman and Klausmeier 2008; Barton et al. 2010). Furthermore, it is often assumed that K_∞ is in a trade-off conflict with the maximum uptake rate, so that an organism is not likely to have a low K_∞ and a high $V_{\max}$ at the same time. Allometric scaling of these traits (Litchman et al. 2007; Edwards et al. 2012) is used in theories predicting optimal cell size (Verdy et al. 2009) and to model community size-structure in microbes (Ward et al. 2012). In large-scale biogeochemical applications, nutrient uptake and growth are often equated, but there is also a rich literature where the two are separated by making cellular growth dependent on internal stores of nutrients (Droop's model). Here, we focus on nutrient uptake mechanisms only.

It was recognized early that measured values of K_∞ are sensitive to environmental variables such as temperature (Goldman and Carpenter 1974) but also to other experimental conditions (Harrison et al. 1989). The uncertainty associated with the assignment of particular values of K_∞ for species and organism groups has led to dissatisfaction with current modeling practice (Franks 2009). Some theoretical studies support the view that the MM half-saturation coefficient is a composite parameter reflecting several sources of variability (Aksnes and Egge 1991; Armstrong 2008; Aksnes and Cao 2011). Furthermore, Pasciak and Gavis (1974) showed that, fundamentally, the V vs. S_∞ relationship is not of a MM functional form in the case of diffusion-limited uptake, and consequently for this case, there is a bias associated with the use of a MM relationship.

Although there are several reasons to reconsider the current use of MM in ecological modeling, its popularity remains strong. The MM model is simple, and measurements of the two coefficients are widely available in the literature. This is in contrast to alternative models that commonly include more than two, less-established coefficients. An important point is that the MM model does not explicitly contain the microbial "master trait" (Litchman and Klausmeier 2008): the size of the organism. This implies that the MM model in an ecological context often requires additional parameterizations and coefficients that describe, e.g., how $V_{\max}$ and K_∞ depend on size and temperature. Such uncertainty in parameterizations can be

* Corresponding author: oyvind.fiksen@bio.uib.no

Table 1. Symbols, descriptions, and units of key variables.

Symbol	Description and unit
a	Uptake affinity of a single uptake site (volume cleared of nutrient molecules for $S_0 \rightarrow 0$ [$m^3\ s^{-1}$])
A	Catchment area of an uptake site (m^2)
α_∞	Uptake affinity of a cell (volume cleared of nutrient molecules for $S_\infty \rightarrow 0$ [$m^3\ cell^{-1}\ s^{-1}$])
α_{max}	Maximum uptake affinity of a cell ($m^3\ cell^{-1}\ s^{-1}$)
$\tilde{\alpha}_\infty$	MM-approximated uptake affinity from $V_{max} : K_\infty$ ($m^3\ cell^{-1}\ s^{-1}$)
α_s	Volume-specific uptake affinity for a cell (α_∞ divided by cell volume [s^{-1}])
β	Dimensionless property from Armstrong (2008)
D	Molecular diffusion coefficient ($m^2\ s^{-1}$)
h	Uptake site handling time (the time a site is occupied after hit by a nutrient molecule [s])
K_0	MM half-saturation coefficient with S_0 as the reference concentration ($mol\ m^{-3}$)
K_∞	Common bulk MM half-saturation coefficient with S_∞ as the reference concentration ($mol\ m^{-3}$)
K_{Q_∞}	Bulk half-saturation coefficient of the quadratic model with S_∞ as the reference concentration ($mol\ m^{-3}$)
$\tilde{K}_\infty$	Bulk half-saturation coefficient of the MM-approximated quadratic model with S_∞ as the reference concentration ($mol\ m^{-3}$)
n	Number of uptake sites per cell
p	Fraction of cell surface area covered by uptake sites
r	Cell radius (m)
s	Uptake site radius (m)
S_0	Substrate concentration at the cell surface ($mol\ m^{-3}$)
S_∞	Substrate concentration outside the boundary layer (here equated with the observed bulk concentration [$mol\ m^{-3}$])
v	Mass transfer coefficient ($m\ s^{-1}$) of Aksnes and Egge (1991)
V	Uptake rate per cell ($molecules\ cell^{-1}\ s^{-1}$)
$\tilde{V}$	Uptake rate from the MM-approximated quadratic model ($molecules\ cell^{-1}\ s^{-1}$)
V_{max}	Maximum uptake rate per cell ($molecules\ cell^{-1}\ s^{-1}$)
$V_{s\ max}$	Volume-specific maximum uptake rate (V_{max} divided by cell volume [$molecules\ m^{-3}\ s^{-1}$])

reduced in models where these properties are embedded mechanistically.

The main objective of the present review is to demonstrate how the MM model and non-MM models, which embrace cell size, in combination can bring trait-based modeling one step further. To achieve this, we summarize some of the proposed MM and non-MM models in order to establish a common framework and terminology. We then point out a line of convergence between different models. Furthermore, we demonstrate weaknesses in the assumed trade-off conflict between the two MM uptake parameters, and we show how non-MM models can provide guidance to identify more specific trait representations and trade-off conflicts than offered by the MM. Finally, we show how estimates of traits specified for structures and processes beyond the experimental bulk (population, container) scale can be obtained from estimates of MM coefficients and uptake affinity.

Methods

History and terminology of some nutrient uptake models—In the enzymatic analogy of microbial nutrient uptake, the role of enzymes is played by transporters or uptake sites. The uptake process is then described by the reaction:

$$S_0 + E_f \xrightarrow{k_1} ES_0 \xrightarrow{k_2} S_i + E_f \tag{2}$$

where S_0 represents the nutrient concentration in the vicinity of the cell surface, E_f is the unoccupied transporter enzyme, k_1 and k_2 are the rate constants, ES_0 is the enzyme-substrate compound, and S_i represents nutrient transport into the cell. By applying the law of mass action, it is possible to deduce an equation for the nutrient uptake rate (Bonachela et al. 2011):

$$V = \frac{k_2 E S_0}{k_2/k_1 + S_0} = \frac{V_{max} S_0}{K_0 + S_0} \tag{3}$$

which is the MM functional form (Eq. 1) with maximum uptake rate, $V_{max} = k_2 E$, and the half-saturation coefficient, $K_0 = k_2/k_1$. Here, S_0 and $E = E_f + ES_0$ are the nutrient concentration at the cell surface and the total number of transporters of a cell, respectively. Note that the half-saturation coefficients of Eq. 1 and Eq. 3 are in general not equal, K_0 is the nutrient concentration near the cell surface, and K_∞ is the bulk concentration measured in experiments or in the ocean. K_0 and K_∞ are equal only for the irrelevant case where there is no boundary layer with decreasing nutrient concentration towards the cell, or no nutrient uptake. The two coefficients are connected through the two processes molecular diffusion and nutrient uptake by the cell, which drive this microscale concentration gradient.

In light of Holling's "disk" equation, a microbe can also be seen as an organism with n uptake sites (corresponding to transporters in the MM model), each with a nutrient catchment area at the cell surface of A (Aksnes and Egge 1991). Handling of nutrient molecules from the outside to the inside of the cell is here assumed to block the site for a period, the handling time h. The uptake rate (V) for the cell is then expressed by a Holling disk equation or functional response II (Holling 1966):

$$V = \frac{nAvS_0}{1 + hAvS_0} \tag{4}$$

where $a = Av$ has the units $m^3\ s^{-1}$ and corresponds to the affinity (*see* below) of a single uptake site, and the mass-transfer coefficient v is affected by molecular diffusion. Rearrangement of Eq. 4 into the MM form (Eq. 3) yields $V_{max} = nh^{-1}$ and $K_0 = (ah)^{-1}$ (Aksnes and Egge 1991). Note that neither this model nor the MM model in Eq. 3 explicitly addresses the boundary layer of the cell.

Due to their small size, microorganisms are generally assumed to be surrounded by a boundary layer with decreasing nutrient concentration toward the cell caused by diffusion-limited flux through this layer (Munk and Riley 1952; Jumars et al. 1993). In this case, the uptake rate of the cell can be taken as being equal to the net flux of nutrient molecules toward the cell, which we assume to be spherical in the following (Pasciak and Gavis 1974; Berg and Purcell 1977; Jumars et al. 1993):

$$V = 4\pi Dr(S_\infty - S_0) \tag{5}$$

where D ($m^2\ s^{-1}$) is the solute's molecular diffusion coefficient, r is cell size (radius, m), S_0 is the nutrient concentration at the cell surface, and S_∞ is the concentration outside the boundary layer, which in practice corresponds to the bulk concentration measured in experiments or the environmental nutrient concentration commonly specified in ecosystem modeling. From Eq. 5, it might appear as if the uptake is driven by the concentration gradient, but in nature it is obviously the other way around. The gradient is driven by the active uptake of the cell, so that S_0 rather than V is the dependent variable. Thus, except for the case when S_0 is zero, this model is unable to predict uptake rate.

If all nutrients encountering the cell surface are immediately absorbed, so that $S_0 = 0$, then $V_{max} = \alpha_{max} S_\infty$, and $\alpha_{max} = 4\pi Dr$ is the volume cleared for nutrients per cell (Table 1). This is the "maximum uptake affinity" (Thingstad et al. 2005; Tambi et al. 2009), a theoretical upper limit for the uptake rate set by the rate of diffusion and the size of the cell. In a crucial step, Berg and Purcell (1977) derived a relationship between V and the number (n) of uptake sites (with substrate capture radius s) for a spherical cell:

$$V = 4\pi Dr(S_\infty - S_0)\frac{ns}{ns + \pi r} \tag{6a}$$

This expression assumes that all molecules hitting an uptake site are absorbed without time delay (they become immediately free to absorb another molecule), which is a reasonable assumption for low external nutrient concentrations. Critically, uptake is dependent on the number of transporters in the cell surface; uptake saturates as the number of transporter sites becomes large. Northrup (1988) tested the model numerically and found some divergence between the analytical model (Eq. 6a) and the numerical simulation at high site coverage, but this discrepancy was eliminated when Zwanzig (1990) introduced a correction term $(1 - p)$ reflecting the interaction between sites:

$$V = 4\pi Dr(S_\infty - S_0)\frac{ns}{ns + \pi r(1-p)} \tag{6b}$$

where p is the fraction of the surface area covered with uptake sites ($n\pi s^2/4\pi r^2$). Equation 6b is therefore a more accurate representation of nutrient uptake than Eq. 6a if uptake sites become immediately free to absorb another molecule after a hit (infinitely small handling time). The uptake affinity (α_∞) of a cell is then (Aksnes and Cao 2011):

$$\alpha_\infty = 4\pi Dr\frac{ns}{ns + \pi r(1-p)} \tag{7}$$

This expression of affinity is derived independently of MM kinetics, and, fundamentally, it does not correspond to the MM affinity given by the ratio $V_{max} : K_\infty$. It defines the affinity of a cell in terms of the inherent traits r and n, in addition to s, which relates to the size of the nutrient molecule and to the molecular diffusion of the solute.

The MM model and diffusion-limited nutrient transport can be coupled. Pasciak and Gavis (1974) combined the MM equation (Eq. 1) with Eq. 5 and obtained a quadratic (non-MM) model of V vs. S_∞. Their approach was revisited by Armstrong (2008), who derived a MM-*approximation* of the quadratic solution for the way in which V relates to S_∞. A Holling approach similar to Aksnes and Egge's (1991) was included to provide relationships between the coefficients of the MM-approximation on one hand and the handling time and number of uptake sites on the other. Uptake rate in the model of Armstrong (his eq. 12) is expressed in units of inverse surface area. Here, we use the versions of Ward et al. (2011, their eq. 3) and more recently Bonachela et al. (2011, their eq. 3), where uptake rate is expressed per cell. Then, for a spherical cell, the MM-approximation of the quadratic model of Armstrong (2008) takes the form ($\tilde{V}$ used for uptake rate to emphasize that it was derived as an approximation):

$$\tilde{V} = nh^{-1}\frac{S_\infty}{K_0 + nh^{-1}(4\pi rD)^{-1} + S_\infty} \tag{8}$$

From Eq. 8, it is clear that $V_{max} = nh^{-1}$ as in the Aksnes and Egge (1991) model, and that the half-saturation coefficient of the MM-approximated quadratic model is:

$$\tilde{K}_\infty = K_0 + nh^{-1}(4\pi rD)^{-1} \tag{9}$$

which was termed the "effective half-saturation constant: in Bonachela et al. (2011). Here, K_0 (denoted k_p in Armstrong 2008) was called the "half saturation constant for site-limited transport." Thus, Armstrong (2008) explicitly differentiated the two half-saturation coefficients, K_0 and $\tilde{K}_\infty$, which are defined according to different reference nutrient concentrations (S_0 and S_∞). Ward et al. (2011, their eq. 15 and eq. 16) and Bonachela et al. (2011, their eq. 5) used Eq. 8 to obtain an expression for the uptake affinity:

$$\begin{aligned}\tilde{\alpha}_\infty = V_{max}/\tilde{K}_\infty &= \frac{nh^{-1}}{K_0 + \dfrac{nh^{-1}}{4\pi rD}} \\ &= \frac{nh^{-1}}{(ah)^{-1} + \dfrac{nh^{-1}}{4\pi rD}} = \frac{4\pi rDna}{4\pi rD + na}\end{aligned} \tag{10}$$

We denote this uptake affinity $\tilde{\alpha}_\infty$ to distinguish it from α_∞ in Eq. 7, as the two quantities are derived differently. Equation 10 contains a composite parameter, a, which can be defined so that $\tilde{\alpha}_\infty$ becomes identical to α_∞ (*see* below). Note that handling time is not part of any definition of uptake affinity. This is because the affinity (the initial slope of the $V:S_\infty$ curve) reflects the response at low resource concentrations, where encounter is the rate-limiting step, not handling.

Aksnes and Cao (2011) applied the results of Berg and Purcell (1977) and Zwanzig (1990) (Eq. 6b above), but since these models have no upper bound on the uptake rate as the substrate concentrations rises, the handling time (h) of an uptake site was introduced. As in Aksnes and Egge (1991), it was assumed that an uptake site is occupied and unable to accept new molecules during the handling time, which led to the following expression for V vs. S_∞:

$$V = \frac{b}{2c}\left(1-\sqrt{1-\frac{4c}{b^2}}\right),$$
$$\text{where } c = \frac{h}{4n\pi rDS_\infty}\left(1-\frac{\pi rp}{ns}\right), \qquad (11)$$
$$\text{and } b = \frac{1}{\alpha_\infty S_\infty}+\frac{h}{n}$$

Similar to the model derived by Pasciak and Gavis (1974), this is also a quadratic and not a MM expression. As in Aksnes and Egge (1991), $V_{\max} = nh^{-1}$, but the affinity (α_∞, in Eq. 7), and not the half-saturation coefficient, appears in this model. The half-saturation coefficient of this quadratic expression, however, is found by setting $V = n/2h$ (uptake rate at 50% of the maximal uptake rate) and $S_\infty = K_{Q_\infty}$ and then solving Eq. 11 for K_{Q_∞} (Aksnes and Cao 2011):

$$K_{Q_\infty} = \frac{\pi r(2-p)+ns}{8h\pi rsD} \qquad (12)$$

While $\tilde{K}_\infty$ is derived by approximating the quadratic solution to the MM functional form (Armstrong 2008), K_{Q_∞} is the half-saturation coefficient of the quadratic model in Eq. 11 and may reflect observed half-saturation coefficients more accurately than $\tilde{K}_\infty$.

The expression for the approximate half-saturation coefficient ($\tilde{K}_\infty$) contains the composite parameter K_0 (Eq. 9). According to Armstrong (2008), $K_0 = (ah)^{-1}$, where $a = 4Ds\beta$ (Armstrong 2008, p. 1314), and β is a dimensionless quantity. It turns out that if we define $\beta = 1/(1-p)$:

$$K_0 = \frac{(1-p)}{4hsD} \qquad (13a)$$

then insertion into Eq. 9 yields:

$$\tilde{K}_\infty = \frac{\pi r(1-p)+ns}{4h\pi rsD} \qquad (13b)$$

which is identical to the expression for the half-saturation coefficient termed MM-approximation 1 (different from Eq. 12) in Aksnes and Cao (2011). Furthermore, if a in Eq. 10 is substituted in the same way, the affinities of Eq. 10 and Eq. 7 become identical ($\tilde{\alpha} = \alpha_\infty$). Another implication of this is that the MM-approximated uptake models of Armstrong (2008) and Aksnes and Cao (2011, their MM-approximation 1) are identical. The expression we defined here, $\beta = 1/(1-p)$, implies that as the density of uptake sites (p) increases, K_0 (the nutrient concentration close to the cell at $V_{\max}/2$) approaches zero. This functional relationship appears reasonable, and we have applied $\beta = 1/(1-p)$ in order to compare the MM-approximated quadratic model with the quadratic model.

Model analyses and parameter estimations—We compared uptake rates obtained by the MM-approximated quadratic model (Eq. 8) with those of the exact solution of the quadratic model (Eq. 11) for different densities of uptake sites (p), different cell sizes (r), and different nutrient concentrations (S_∞). The differences between the two models were calculated as the ratio $(V-\tilde{V})/V$.

While V, $V_{\max}$, and α_∞ represent absolute rates per cell, we will also make use of specific rates, or the uptake rate per cell volume. They were obtained by dividing absolute rates by cell volume, $(4/3)\pi r^3$ (still assuming a sphere), a proxy for cell mass or quota. Furthermore, instead of the number of uptake sites (n), we specify the density of uptake sites ($p = n\pi s^2/4\pi r^2$) so that $n = 4pr^2s^{-2}$. Thus, the volume-specific maximum uptake rate ($V_{s\ \max}$, $\mathrm{m^{-3}\ s^{-1}}$) and the specific affinity (α_s, $\mathrm{s^{-1}}$) are:

$$V_{s\max} = \frac{V_{\max}}{\frac{4}{3}\pi r^3} = \frac{4pr^2s^{-2}}{h\frac{4}{3}\pi r^3} = \frac{3p}{\pi hs^2r} \qquad (14)$$

$$\alpha_s = \frac{\alpha_\infty}{\frac{4}{3}\pi r^3} = \frac{4\pi Drns}{(ns+\pi r(1-p))\frac{4}{3}\pi r^3} = \frac{12Dp}{(4rp+\pi s(1-p))r} \qquad (15)$$

We will use Eq. 14 to predict how the uptake site density p (through n), organism size r, and handling time h affect the maximum uptake rate, and α_s will be used as index of competitive strength of an organism at low nutrient concentrations (Thingstad et al. 2010).

Microbial traits can be estimated from measurements of $V_{\max}$, K_∞, and α_s. If the size of an organism (r) and the value of the molecular diffusion (D) of the solute are known, we are left with three unknowns, n, s, and h (p is given by n, s, and r) and three equations that connect these traits to $V_{\max}$, K_∞, and α_s (Eq. 7, Eq. 12, and the relationship $V_{\max} = nh^{-1}$). Here, we have estimated n and h from the measurements of $V_{\max}$, K_∞, and r by insertion of $n = hV_{\max}$ in Eq. 12 and solving for h:

$$h = 2\pi r/(\pi V_{\max}\frac{s^2}{4r} - V_{\max}s + 8\pi K_\infty Drs) \qquad (16)$$

The value of s was approximated as 0.001 μm (Berg and Purcell 1977) and D with 1000 $\mu\mathrm{m^2\ s^{-1}}$. We have used observations of $V_{\max}$ and K_∞ from single species that are reported in Litchman et al. (2007) and from allometric scaling of $V_{\max}$ and K_∞ for nitrogen and phosphorus uptake reported in Edwards et al. (2012).

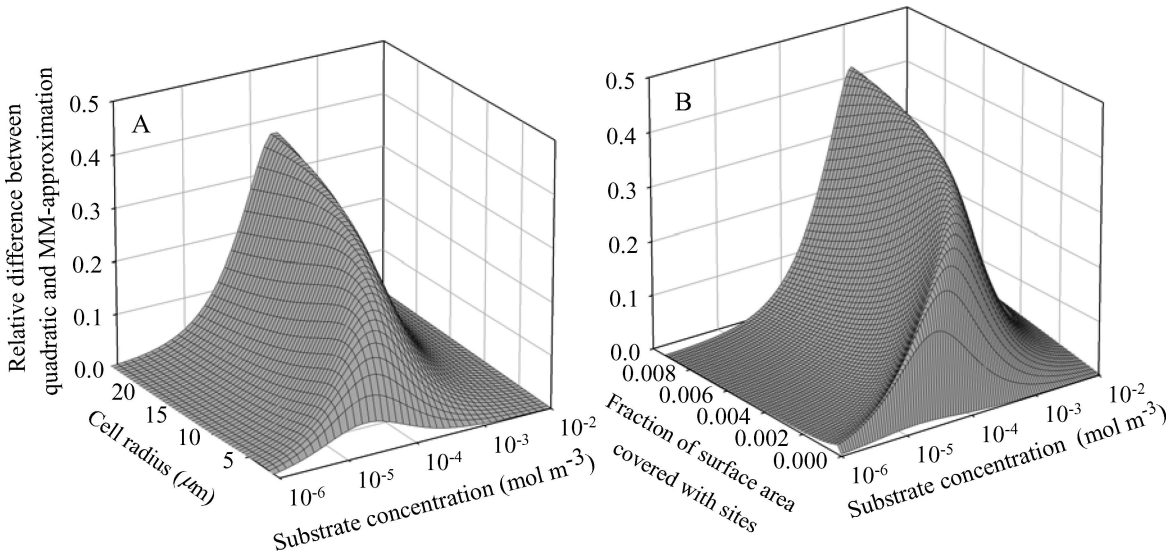

Fig. 1. The relative difference between the MM-approximated, $\tilde{V}$ (Eq. 8) and the exact quadratic solution V (Eq. 11) for (A) substrate concentration S_∞ and cell size assuming fixed site density (p) corresponding to 0.00048; (B) over site density and substrate concentration (5 μm radius).

Results

Bias of the MM-approximated quadratic model for uptake rate—The relative difference between the MM-approximation (Eq. 8) and the exact solution of the quadratic model for nutrient uptake rate ($[V - \tilde{V}]/V$) is minor at low and high substrate concentrations (Fig. 1). This is not surprising because the uptake rates at the two substrate limits, where S_∞ is 0 or ∞, are determined by the expressions of affinity and $V_{\max}$, respectively, and assuming $\beta = 1/(1 - p)$ (*see* Methods), these two limits are identical in the models. Consequently, because the MM-approximated half-saturation coefficient is different from that of the exact quadratic model, the difference between the two models peaks at nutrient concentrations around K_∞ (Fig. 1), where the MM-approximated model provides uptake rates that are up to 50% lower than the exact solution.

Organism size and uptake site density as master traits—Both the MM approximation and the exact quadratic model suggest that increased density of uptake sites (p), will increase both the specific maximum uptake rate (Eq. 14) and the bulk half-saturation coefficient (Eq. 12 and Eq. 13b; Fig. 2). Cell radius r increases K_∞ and reduces $V_{s\ \max}$ and is another candidate to generate covariation between the two. Interestingly, variations in r and p cause opposite relationships between $V_{s\ \max}$ and K_∞. Increasing size yields a negative relationship between $V_{s\ \max}$ and K_∞, and smaller cells will always have higher $V_{s\ \max}$ and lower K_∞ relative to larger cells (Fig. 2). When we combine reasonable values of r and p at random, no correlation between $V_{s\ \max}$ and K_∞ appears, except that a narrowing range of $V_{s\ \max}$ at higher K_∞ is evident (Fig. 2). The model predicts that K_∞ and $V_{s\ \max}$ are not likely to be correlated if species vary in the size–uptake site density space. If we use the exact solution instead of the MM approximation, the patterns are similar, although the numerical values differ slightly (steeper curves, not shown).

Low K_0 *and high* α_∞*, but not* K_∞*, are indices of uptake ability*—Increasing site density increases K_∞, as well as $\tilde{K}_\infty$, linearly (Fig. 2), which is a rather surprising result if high K_∞ is considered to characterize a poor competitor under low nutrient concentrations. Here, a higher K_∞ instead means a stronger competitor at low nutrient concentration, since more uptake sites always increase the uptake rate. This result applies to the K_∞ of both the MM approximation (Eq. 13b) and the exact quadratic model (Eq. 14). Interestingly, a different result is obtained for K_0. Increased p in Eq. 13a *decreases* K_0 according to the factor $1 - p$. Although this decrease in K_0 with increased p is not very pronounced for low values of p, this sensitivity of K_0 is consistent with the common interpretation that a lower value enhances the competitive ability at low substrate concentrations. However, this result is of little practical interest as measurements of K_0 require observations of S_0. The affinity, however, is a direct measurement of the uptake ability, and thereby the competitive strength, at low S_∞. Specific affinity (Eq. 15) increases with site density and decreases with size (Fig. 3A). The decrease with lowered density of uptake sites is in accordance with the expectation of reduced uptake ability at low substrate concentration.

A trade-off conflict between maximum uptake rate and the half-saturation coefficient?—A trade-off is present when a trait is beneficial for one function but gives a disadvantage for another function (Litchman and Klausmeier 2008). Uptake V increases monotonically with p over all S_∞ (Fig. 3B); therefore, the simultaneous increase of both K_∞ and $V_{s\ \max}$ with p as illustrated in Fig. 2 and Fig. 3C is not a trade-off conflict because more uptake sites will always increase the rate of uptake (Fig. 3B).

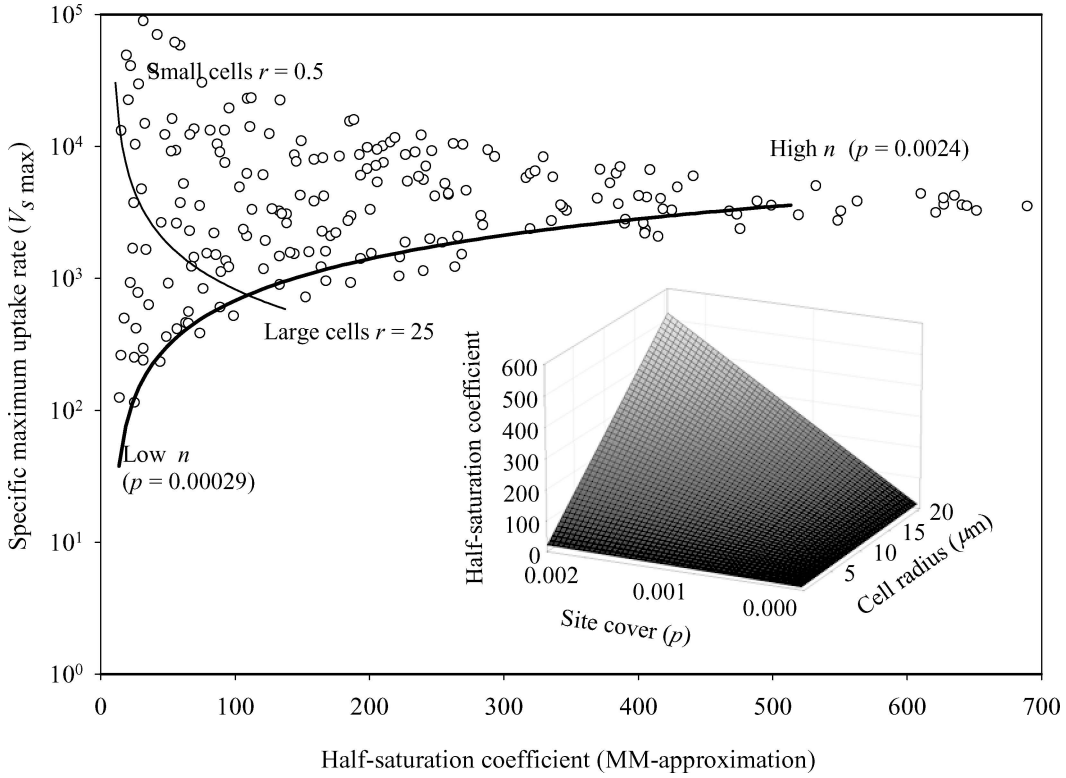

Fig. 2. The maximum specific uptake $V_{s\,max}$ (Eq. 14) vs. the bulk half-saturation coefficient, K_∞ (Eq. 13b). The changes in K_∞ and $V_{s\,max}$ were obtained by increasing either the number of uptake sites n (bold line) and keeping radius fixed (r = 20 μm), or by increasing r while keeping uptake sites fixed (n = 476, thin line). We also drew p and r randomly from uniform distributions with the range of r from 0.5 to 20 μm and range of n densities (p = 0.05 to 5 times 0.00048, the density estimated for *Vibrio splendidus* by Aksnes and Cao 2011; dots). The inset figure shows how K_∞ increases with cell size r and with fraction of surface covered by sites (p). We used handling time h = 0.03 s and not 0.12 s as in Aksnes and Cao (2011) because of an error in their estimate.

Handling time and nutrient uptake—Handling time can be a direct link between the efficiency of the interior machinery of a cell and the uptake rate (Aksnes and Egge 1991). We illustrate this for a case where both handling time and the density of uptake sites are reduced (Fig. 3D, gray line). With low handling time, this cell will be more efficient at high nutrient concentrations, even with far fewer uptake sites.

Estimates of site density and handling time—Estimates of h and p (*see* Methods) from data on K_∞ and $V_{\max}$ by Litchman et al. (2007) show that both traits were negatively correlated with cell radius (Fig. 4A; h: $R^2 = 0.49$, $p < 0.01$, p: $R^2 = 0.4$, $p < 0.01$). The specific affinity (α_s) resulting from these values of r and p (Eq. 15) is dominated by the effect of cell radius. The same general pattern of decreasing h, p, and α_s with cell size is found when we apply data from the recent review by Edwards et al. (2012). By use of the allometric scaling of K_∞ and $V_{\max}$ for freshwater and marine species combined (in their table 1), we find the resulting allometric relationships and scaling coefficients for handling time, uptake site coverage, and specific affinity for nitrate and phosphorus (Fig. 4B).

Discussion

Traits and trade-offs in nutrient uptake—Ecological competition theory (Tilman 1977; Tilman et al. 1982) and biogeochemical modeling (Barton et al. 2010) often adopt a MM or Monod kinetics framework to trait-based approaches (Litchman and Klausmeier 2008; Follows and Dutkiewicz 2011). The MM approach is also simple and convenient for a range of applications with intensive computational demands, but it does not account explicitly for diffusion limitation (Pasciak and Gavis 1974; Armstrong 2008) and, therefore, may not be entirely accurate (Fig. 1). Furthermore, from the analysis presented here, we were not able to identify any mechanistic trade-off conflicts between the specific maximum uptake rate and the half-saturation constant. In the MM-tradition (Eq. 1), $V_{s\,max}$ and K_∞ are often assumed to be in a trade-off relationship—some organisms are good at growing fast at high nutrient levels (high $V_{s\,max}$), while others are better competitors at low nutrient concentrations and have low K_∞. Our results suggest that a higher uptake site density will increase both the specific maximum uptake rate, which is a proxy for maximum growth rate, and the bulk half-saturation coefficient K_∞ (Eq. 11a,b; Fig. 2) at any substrate density and cell size. Thus, increased K_∞ is associated with increased competitive ability for all nutrient concentrations.

If the density of uptake sites at the cell surface is held constant, then K_∞ will increase with cell size r, and the higher K_∞ is followed by a lower specific maximum uptake rate (Fig. 2, thin line). This implies that smaller cells are better competitors at all nutrient concentrations. Naturally, larger cells will have a higher uptake rate per cell ($V_{\max}$),

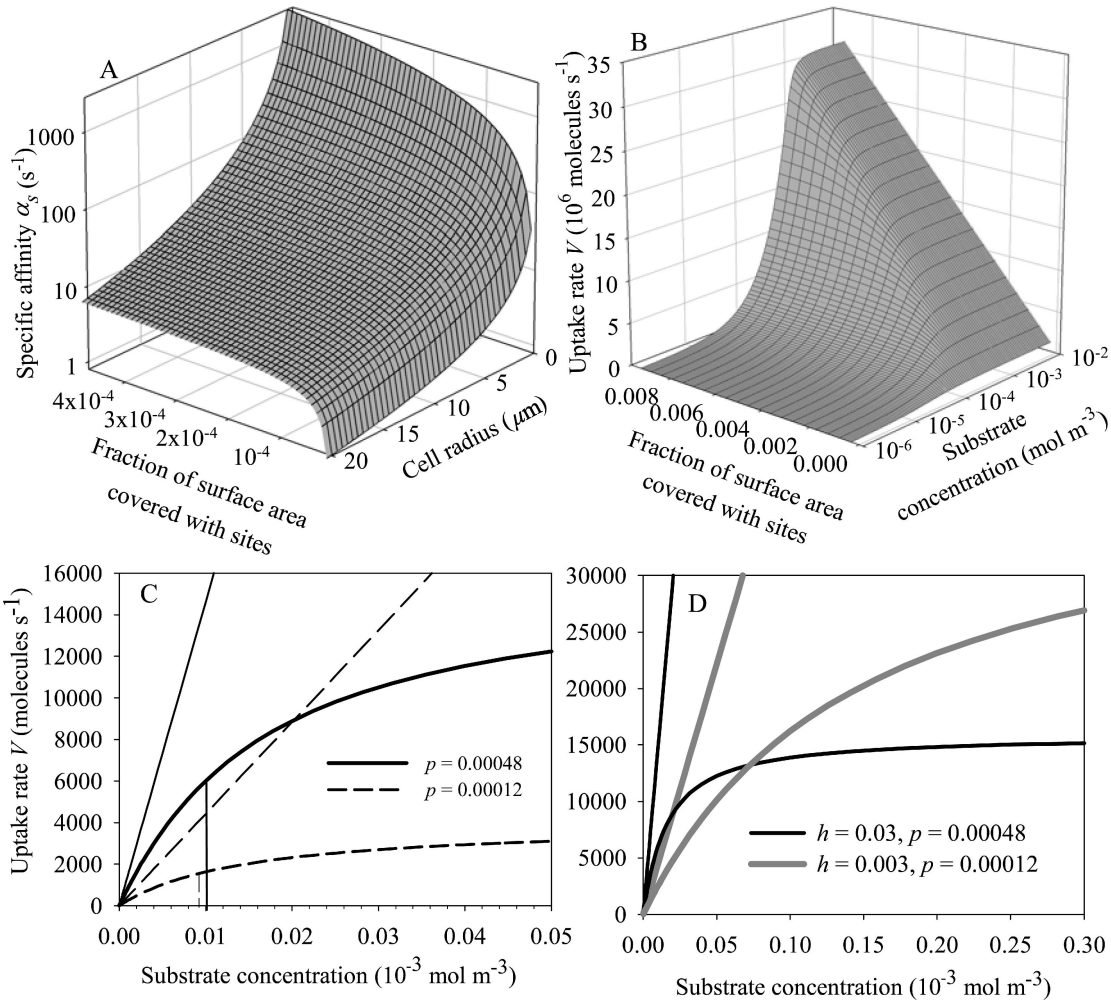

Fig. 3. (A) Specific affinity α_s (Eq. 15) as a function of uptake site cover (p) and cell radius (r). (B) Uptake (r = 5 m) as a function of substrate concentration and uptake site cover. (C) Uptake rate (Eq. 11) for two small cells (r = 0.5 m, h = 0.03 s) as a function of substrate concentration, where site densities differ by a factor of four. Straight lines indicate affinities as the initial slope of the curves ($m^3\ s^{-1}$; Eq. 7) for each cell, and the vertical lines indicate the corresponding half-saturation coefficient ($K_{Q\infty}$; Eq. 12). (D) Uptake rate for a cell with lower handling time and fewer uptake sites (gray line), while the continuous black lines are the same as in panel C.

but this can hardly be interpreted as determinant for competition unless other internal allometries are involved. The maximum uptake rate $V_{\max}$ is a direct effect of size because $V_{\max} = nh^{-1} = 4pr^2s^{-2}h^{-1}$, and therefore $V_{\max}$ (but not $V_{s\ \max}$) will be correlated with K_∞ over cell size. This is also evident in the data presented by Litchman et al. (2007, their fig. 1a,b).

An increasing density of uptake sites (Fig. 2, fat line) increases both $V_{s\ \max}$ and K_∞, although K_0 appears to decrease slightly with p (Eq. 13a). Site density p and cell radius r thus have opposite effects on the relationship between specific maximum uptake rate and K_∞. We suspect this explains why there appears to be no relationship between maximum specific uptake rate and estimated K_∞ from the empirical data compiled by Litchman et al. (2007, their fig. 1b).

Specific uptake affinity and competitive strength under oligotrophic conditions—Specific affinity integrates the two master traits (r, n) for uptake rate at low nutrient concentrations and therefore grades competitive ability of organisms in the oligotrophic situation. It specifies the volume cleared for nutrients (per time and cell volume) when S_∞ approaches zero. Several earlier studies (Healey 1980; Smith et al. 2009; Aksnes and Cao 2011) have pointed at affinity as a more appropriate index for uptake ability at low substrate concentration than K_∞. Lack of discrimination of S_0 from S_∞, K_0 from K_∞, and α_0 from α_∞ has led to expressions where affinity appears proportional to n (Aksnes and Egge 1991; Smith et al. 2009). In our framework, setting $\alpha_0 = nh^{-1}/K_0$ gives $\alpha_0 = 4Dsn/(1 - p)$ by use of Eq. 13a, which does increase (for small p) linearly with n, while α_∞ saturates rapidly with site coverage. However, similar to K_0, α_0 is not a very useful experimental quantity because it is defined according to the unknown nutrient concentration at the cell surface (S_0).

Maximum uptake rate (Eq. 14) is proportional to site density and therefore a better candidate than α_∞ to be in a trade-off for material or fuel with the internal cellular machinery to process nutrient molecules. This is in contrast to the optimal uptake kinetics (OU) models

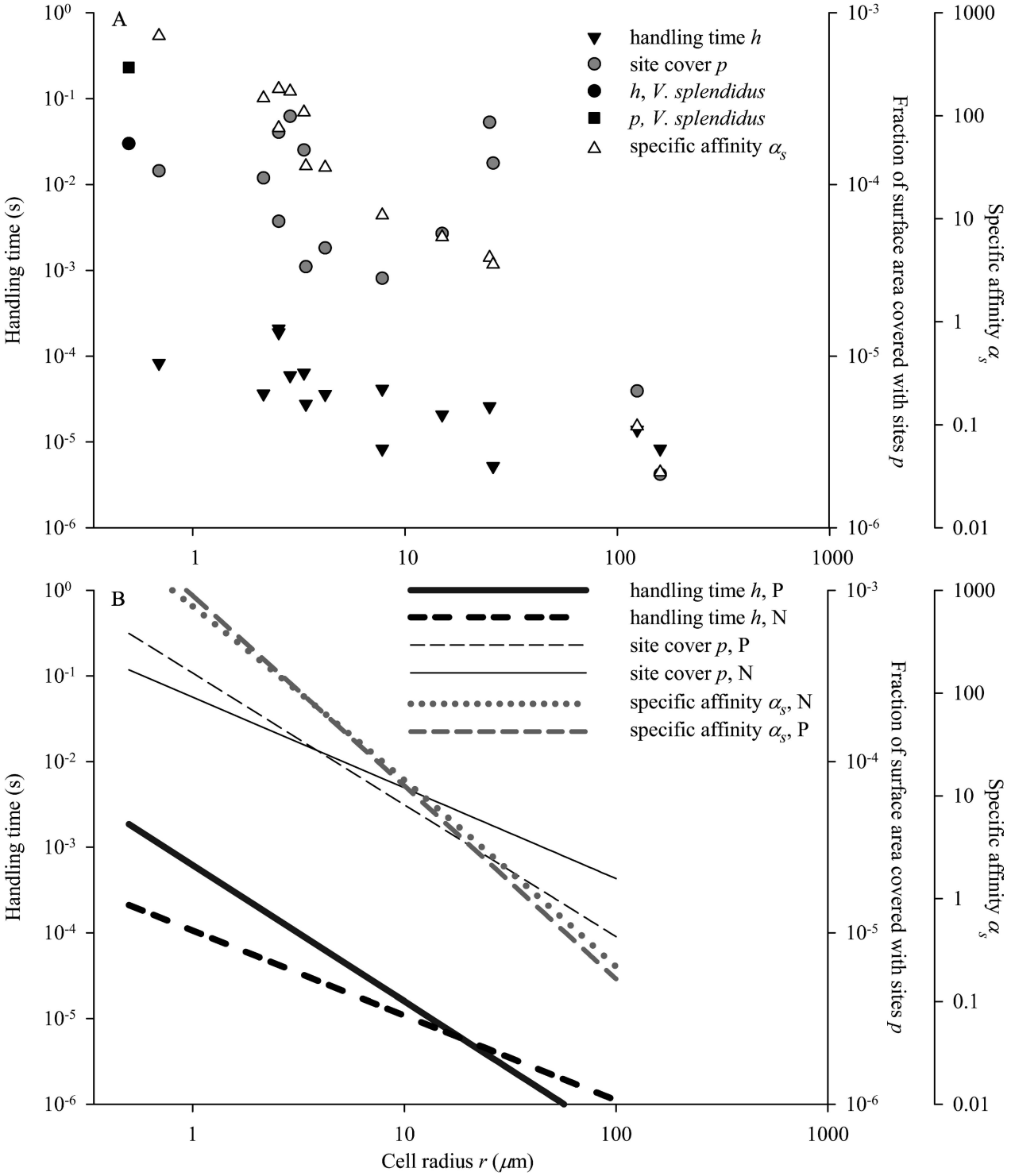

Fig. 4. (A) Handling time h from Eq. 16 and fraction of surface covered with uptake sites p as a function of cell radius based on estimates of r, V_{max}, and K_∞ compiled by Litchman et al. (2007). The data represent uptake of nitrate in different algal groups. We used the values of h and p to calculate individual specific affinity α_s (s^{-1}; Eq. 15). The values for the bacterium *Vibrio splendidus* consuming phosphate are from Aksnes and Cao (2011). (B) The allometric scaling of handling time h (thick black lines), site cover p (thin black lines), and specific affinity (gray lines) for uptake of nitrate (N) and phosphate (P) from the recent review of scaling in V_{max} and K_∞ by Edwards et al. (2012, their table 1). The allometric scaling slopes (based on cell volume in μm^3) for handling time are -0.33 (N) and -0.53 (P) and for site cover -0.18 (N) and -0.26 (P).

(Smith and Yamanaka 2007; Smith et al. 2009), which assume that affinity is proportional to uptake site density. OU models do not explicitly include diffusion limitation, which implies the assumption that $S_0 = S_\infty$ and consequently $\alpha_0 = \alpha_\infty$, letting resources be allocated either to sites or to internal processing machinery, which then leads to an affinity vs. maximum uptake trade-off. Bringing diffusion into the equation suggests instead that affinity satiates quickly with site density (Eq. 7 and Eq. 15; Fig. 3A). The assumed trade-off between internal and external hardware in OU models does not appear when diffusion is included. First, more uptake sites increase both α_s and $V_{\max}$, so there is no direct trade-off conflict between these properties through uptake sites. Second, if there is a resource-based trade-off between intracellular machinery and uptake sites, it should instead be linked mechanistically to uptake rate through the handling time h, since a larger internal processing capacity may reduce the time that sites are blocked (Aksnes and Egge 1991).

An improved theoretical framework for nutrient uptake—We have rephrased K_∞ and $V_{s\,\max}$ in terms that may appear to require a larger number of parameters, each of which involves some uncertainty in estimation. We think this is warranted. The size (r) of a microbe is an essential trait in competition theory that is not embraced by the MM model. This framework facilitates an explicit representation of size. In order to relate the two MM parameters to size, this model requires typically two to four additional parameters that may be estimated from nonlinear regressions, or taken from assumed scaling relationships, of the two MM parameters vs. size (Ward et al. 2012). Thus, in models where organism size is embedded, the MM approach is likely to be less efficient, in terms of the number of parameters that must be determined, than the mechanistic framework discussed here. Also, diffusion (salinity, molecular size, and temperature) is not an explicit part of the MM approach, but it is an important property in the viscous environment of the microbial world and a crucial component of the half-saturation and the affinity parameters. This explicit dependence of these two quantities on an environmental property led Aksnes and Cao (2011) to characterize them as apparent, and not inherent, organism traits. In addition to organism size and molecular diffusion, the extended framework discussed here leaves us with n, h, and s instead of the traditional K_∞ and $V_{s\,\max}$. Of them, the radius of the uptake site s is basically a chemical parameter, likely specific to each nutrient and its molecular size. The two traits n (or the uptake site density p) and h can be calculated from experimental values of K_∞, $V_{\max}$, and α_∞ (Fig. 4). Note, however, that according to the quadratic model, it is Eq. 12 (and not 13) that should be used to interpret the nutrient concentration at half the maximum uptake rate. Also, note the α_∞ is fundamentally a non-MM coefficient that should be measured independently of K_∞ and $V_{\max}$ (Thingstad et al. 2005).

Environmental effects on uptake—An analysis of competitive interactions based on mechanistic process formulations yields richer predictions and connects better with environmental variables. For instance, the diffusion process can be parameterized as a physical process driven by temperature, salinity, and molecular size:

$$D = \frac{k_B T}{6\pi\mu R} \tag{17}$$

where k_B is Boltzmann's constant, T is temperature in Kelvin, μ is dynamic viscosity, and R is the molecular radius of the solute (Jumars et al. 1993), which is likely to correlate with the radius of the uptake site, s. Thus, Eq. 17 can be inserted into Eq. 7 to derive expectations of how the uptake affinity responds to temperature and molecular size. In addition, temperature will influence handling time exponentially since it is a physiological process (Aksnes and Cao 2011), while diffusion is quite proportional to temperature. Since diffusion is limiting at low nutrient levels, and handling time is limiting at high nutrient levels, the temperature effect on uptake rate could be different for these cases.

What are the trade-offs?—A remaining challenge is to understand the trade-offs involved with small cell size, high site density, and low handling time. Jumars et al. (1993) pointed out that nutrient uptake saturates at low site coverage, and that the maintenance costs of sites will be an important factor in determining the optimal uptake site density. We still need estimates of production and maintenance costs of sites to know how costly they are relative to alternative use in the cell. Other trade-offs, such as viral infection through uptake sites (Rothenberg et al. 2011), could be an additional adaptive reason to limit their density. The handling time may be linked to internal processes of a cell where idle enzymes or transporters are needed to free the uptake site for the substrate molecule, or other internal bottlenecks. Indeed, both the handling time and the number of uptake sites (Franks 2009) may be quite flexible and vary as a function of environmental conditions. The theory presented here can be tailored to incorporate such plasticity once the trade-offs become clearer. Our reformulation of the data from Litchman et al. (2007) and the recent review by Edwards et al. (2012) suggests a trend of lower coverage of sites and shorter handling time in larger cells. An interesting speculation is that the allometric decline in handling time is related to a more efficient internal transport system in larger cells. Similarly, the specific affinity of larger cells levels off faster with site coverage than that of smaller cells (Fig. 3A). Diminishing return with cell size may be one reason larger cells have lower site density, particularly if there are additional costs associated with the sites. Shorter handling times can also make large cells more competitive under eutrophic conditions (Fig. 3B).

The recent shift to trait-based modeling benefits from mechanistic derivations of the trade-offs (Follows and Dutkiewicz 2011; Smith et al. 2011). The evidence provided here suggests, regardless of model choice (i.e., the MM approximation or the quadratic model), that the MM coefficients measured in experiments using Eq. 1 do not provide a suitable framework for deriving microbial trade-off conflicts unless they are connected to their underlying biological and physical properties, although they are indeed useful to characterize the outcome of experiments. In

conclusion, competition theory and trait-based approaches of nutrient uptake in microbes will benefit from an extended framework where such measurements are interpreted explicitly in terms of inherent organism traits, such as r and n, and physical factors, such as D and T.

Acknowledgments

We thank Stephanie Dutkiewicz, Zoe Finkel, Andrew Irwin, Ben Ward, and two reviewers for comments on an earlier draft, and the Research Council of Norway for project funding, including a sabbatical visit for Ø.F. to the Massachusetts Institute of Technology.

References

Aksnes, D. L., and F. J. Cao. 2011. Inherent and apparent traits in microbial nutrient uptake. Mar. Ecol. Prog. Ser. **440:** 41–51, doi:10.3354/meps09355

———, and J. K. Egge. 1991. A theoretical model for nutrient uptake in phytoplankton. Mar. Ecol. Prog. Ser. **70:** 65–72, doi:10.3354/meps070065

Armstrong, R. A. 2008. Nutrient uptake rate as a function of cell size and surface transporter density: A Michaelis-like approximation to the model of Pasciak and Gavis. Deep-Sea Res. I **55:** 1311–1317, doi:10.1016/j.dsr.2008.05.004

Barton, A. D., S. Dutkiewicz, G. Flierl, J. Bragg, and M. J. Follows. 2010. Patterns of diversity in marine phytoplankton. Science **327:** 1509–1511, doi:10.1126/science.1184961

Berg, H. C., and E. M. Purcell. 1977. Physics of chemoreception. Biophys. J. **20:** 193–219, doi:10.1016/S0006-3495(77)85544-6

Bonachela, J. A., M. Raghib, and S. A. Levin. 2011. Dynamic model of flexible phytoplankton nutrient uptake. P. Natl. Acad. Sci. USA **108:** 20633–20638, doi:10.1073/pnas.1118012108

Dugdale, R. C. 1967. Nutrient limitation in the sea—dynamics, identification and significance. Limnol. Oceanogr. **12:** 685–695, doi:10.4319/lo.1967.12.4.0685

Edwards, K. F., M. K. Thomas, C. A. Klausmeier, and E. Litchman. 2012. Allometric scaling and taxonomic variation in nutrient utilization traits and maximum growth rate of phytoplankton. Limnol. Oceanogr. **57:** 554–566, doi:10.4319/lo.2012.57.2.0554

Follows, M. J., and S. Dutkiewicz. 2011. Modeling diverse communities of marine microbes. Annu. Rev. Mar. Sci. **3:** 427–451, doi:10.1146/annurev-marine-120709-142848

Franks, P. J. S. 2009. Planktonic ecosystem models: Perplexing parameterizations and a failure to fail. J. Plankton Res. **31:** 1299–1306, doi:10.1093/plankt/fbp069

Goldman, J. C., and E. J. Carpenter. 1974. Kinetic approach to effect of temperature on algal growth. Limnol. Oceanogr. **19:** 756–766, doi:10.4319/lo.1974.19.5.0756

Harrison, P. J., J. S. Parslow, and H. L. Conway. 1989. Determination of nutrient uptake kinetic parameters: A comparison of methods. Mar. Ecol. Prog. Ser. **52:** 301–312, doi:10.3354/meps052301

Healey, F. P. 1980. Slope of the Monod equation as an indicator of advantage in nutrient competition. Microb. Ecol. **5:** 281–286, doi:10.1007/BF02020335

Holling, C. S. 1966. The functional response of invertebrate predators to prey density. Mem. Entomol. Soc. Can. **48:** 1–86, doi:10.4039/entm9848fv

Jumars, P. A., J. W. Deming, P. S. Hill, L. Karp-Boss, P. L. Yager, and W. B. Dade. 1993. Physical constraints on marine osmotrophy in an optimal foraging context. Mar. Microb. Food Webs **7:** 121–159.

Litchman, E., and C. A. Klausmeier. 2008. Trait-based community ecology of phytoplankton. Annu. Rev. Ecol. Evol. Syst. **39:** 615–639, doi:10.1146/annurev.ecolsys.39.110707.173549

———, ———, O. M. Schofield, and P. G. Falkowski. 2007. The role of functional traits and trade-offs in structuring phytoplankton communities: Scaling from cellular to ecosystem level. Ecol. Lett. **10:** 1170–1181, doi:10.1111/j.1461-0248.2007.01117.x

Monod, J. 1949. The growth of bacterial cultures. Annu. Rev. Microbiol. **3:** 371–394, doi:10.1146/annurev.mi.03.100149.002103

Munk, W. H., and G. A. Riley. 1952. Absorption of nutrients by aquatic plants. J. Mar. Res. **11:** 215–240.

Northrup, S. H. 1988. Diffusion-controlled ligand-binding to multiple competing cell-bound receptors. J. Phys. Chem.-US **92:** 5847–5850, doi:10.1021/j100331a060

Pasciak, W. J., and J. Gavis. 1974. Transport limitation of nutrient uptake in phytoplankton. Limnol. Oceanogr. **19:** 881–898, doi:10.4319/lo.1974.19.6.0881

Rothenberg, E., L. A. Sepulveda, S. O. Skinner, L. Y. Zeng, P. R. Selvin, and I. Golding. 2011. Single-virus tracking reveals a spatial receptor-dependent search mechanism. Biophys. J. **100:** 2875–2882, doi:10.1016/j.bpj.2011.05.014

Smith, S. L., M. Pahlow, A. Merico, and K. W. Wirtz. 2011. Optimality-based modeling of planktonic organisms. Limnol. Oceanogr. **56:** 2080–2094, doi:10.4319/lo.2011.56.6.2080

———, and Y. Yamanaka. 2007. Optimization-based model of multinutrient uptake kinetics. Limnol. Oceanogr. **52:** 1545–1558, doi:10.4319/lo.2007.52.4.1545

———, ———, M. Pahlow, and A. Oschlies. 2009. Optimal uptake kinetics: Physiological acclimation explains the pattern of nitrate uptake by phytoplankton in the ocean. Mar. Ecol. Prog. Ser. **384:** 1–12, doi:10.3354/meps08022

Tambi, H., G. A. F. Flaten, J. K. Egge, G. Bodtker, A. Jacobsen, and T. F. Thingstad. 2009. Relationship between phosphate affinities and cell size and shape in various bacteria and phytoplankton. Aquat. Microb. Ecol. **57:** 311–320, doi:10.3354/ame01369

Thingstad, T. F., L. Øvreås, J. K. Egge, T. Løvdal, and M. Heldal. 2005. Use of non-limiting substrates to increase size; a generic strategy to simultaneously optimize uptake and minimize predation in pelagic osmotrophs? Ecol. Lett. **8:** 675–682, doi:10.1111/j.1461-0248.2005.00768.x

———, E. Strand, and A. Larsen. 2010. Stepwise building of plankton functional type (PFT) models: A feasible route to complex models? Prog. Oceanogr. **84:** 6–15, doi:10.1016/j.pocean.2009.09.001

Tilman, D. 1977. Resource competition between planktonic algae—experimental and theoretical approach. Ecol. **58:** 338–348, doi:10.2307/1935608

———, S. S. Kilham, and P. Kilham. 1982. Phytoplankton community ecology—the role of limiting nutrients. Ann. Rev. Ecol. Syst. **13:** 349–372, doi:10.1146/annurev.es.13.110182.002025

Verdy, A., M. J. Follows, and G. Flierl. 2009. Optimal phytoplankton cell size in an allometric model. Mar. Ecol. Prog. Ser. **379:** 1–12, doi:10.3354/meps07909

Ward, B., S. Dutkiewicz, A. D. Barton, and M. J. Follows. 2011. Biophysical aspects of resource acquisition and competition in algal mixotrophs. Am. Nat. **178:** 98–112, doi:10.1086/660284

———, ———, O. Jahn, and M. J. Follows. 2012. A size-structured food-web model for the global ocean. Limnol. Oceanogr. **57:** 1877–1891, doi:10.4319/lo.2012.57.6.1877

Zwanzig, R. 1990. Diffusion-controlled ligand-binding to spheres partially covered by receptors—an effective medium treatment. P. Natl. Acad. Sci. USA **87:** 5856–5857, doi:10.1073/pnas.87.15.5856

Associate editor: Heidi M. Sosik

Received: 20 June 2012
Accepted: 05 September 2012
Amended: 10 September 2012